LEVEL II

12

AD A104682

AD

CONTRACT REPORT ARBRL-CR-00461

AN UNSTEADY TAYLOR ANGLE FORMULA FOR LINER COLLAPSE

DTIC ELECTE SEP 29 1981 S H D

Prepared by

Dyna East Corporation
227 Hemlock Road
Wynnewood, PA 19096

August 1981

US ARMY ARMAMENT RESEARCH AND DEVELOPMENT COMMAND
BALLISTIC RESEARCH LABORATORY
ABERDEEN PROVING GROUND, MARYLAND

Approved for public release; distribution unlimited.

81 9 28 157

UNCLASSIFIED

SECURITY CLASSIFICATION OF THIS PAGE (When Data Entered)

REPORT DOCUMENTATION PAGE

READ INSTRUCTIONS BEFORE COMPLETING FORM

1. REPORT NUMBER: CONTRACT REPORT ARBRL-CR-00461	2. GOVT ACCESSION NO.: AD-A104 682
3. RECIPIENT'S CATALOG NUMBER:	
4. TITLE (and Subtitle): An Unsteady Taylor Angle Formula for Liner Collapse	5. TYPE OF REPORT & PERIOD COVERED: Final Rept.
	6. PERFORMING ORG. REPORT NUMBER: Technical Rept. DE-TR-81-1C
7. AUTHOR(s): Pei Chi Chou, Eitan Hirsch, Robert D. Ciccarelli	8. CONTRACT OR GRANT NUMBER(s): DAAK11-79-C-0124
9. PERFORMING ORGANIZATION NAME AND ADDRESS: Dyna East Corporation, 227 Hemlock Road, Wynnewood, PA 19096	10. PROGRAM ELEMENT, PROJECT, TASK AREA & WORK UNIT NUMBERS
11. CONTROLLING OFFICE NAME AND ADDRESS: U.S. Army Armament Research & Development Command, U.S. Army Ballistic Research Lab. (DRDAR-BL), Aberdeen Proving Ground, MD 21005	12. REPORT DATE: AUGUST 1981
	13. NUMBER OF PAGES: 42
14. MONITORING AGENCY NAME & ADDRESS (if different from Controlling Office)	15. SECURITY CLASS. (of this report): Unclassified
	15a. DECLASSIFICATION/DOWNGRADING SCHEDULE: N/A

16. DISTRIBUTION STATEMENT (of this Report)

Approved for public release; distribution unlimited.

17. DISTRIBUTION STATEMENT (of the abstract entered in Block 20, if different from Report)

18. SUPPLEMENTARY NOTES

19. KEY WORDS (Continue on reverse side if necessary and identify by block number)

Explosive-Metal Interaction
Conical Shaped Charge
Exploding Cylinder
Collapse Angle
Taylor Angle
Liner Collapse

20. ABSTRACT (Continue on reverse side if necessary and identify by block number)

An analytical formula for determining the direction of motion for an explosively driven metal liner under unsteady conditions is presented. This direction is defined by the angle δ between the velocity vector of the liner element and the perpendicular to the initial liner surface.

A formula for determining the angle δ was first proposed by G.I. Taylor as $\sin\delta = V/2U$, where V is the final liner element velocity and U is the velocity

DD FORM 1473, 1 JAN 73 — EDITION OF 1 NOV 65 IS OBSOLETE

S/N 0102-014-6601

UNCLASSIFIED

SECURITY CLASSIFICATION OF THIS PAGE (When Data Entered)

387309

by which the detonation wave front sweeps past the liner. This formula is, however, accurate only under steady-state conditions where the detonation wave sweeps past identical cross sections of the explosive-liner geometry. For non-steady cases, the Taylor formula is not applicable since the existence of a velocity gradient or a gradient of the typical acceleration duration along the liner may significantly affect the angle δ.

The new formula is tested against both numerical calculations and experimental data and predicts the angle δ more accurately than the steady Taylor formula.

The derivation of the formula along with a comparison of its predictions for the angle δ with previous experimental work and two-dimensional code calculations for both a conical-shaped charge and exploding cylinder are presented in this report.

FOREWORD

This report represents Part C of a four-part final report for Contract No. DAAK11-79-C-0124. These four parts address the topics: (A) "Maximum Jet Velocity and Comparison of Jet Breakup Models"; (B) "The Virtual Origin Approximation in Hemi Charges and Shaped Charges"; (C) "An Unsteady Taylor Angle Formula for Liner Collapse"; and (D) "Jet Formation of an Implosively Loaded Hemispherical Liner." Each part is bound separately for convenience.

Table of Contents

List of Illustrations

I. Introduction

When a metal liner is driven to a velocity V by an explosive charge, it is often important to know not only the magnitude of its velocity but also the direction in which each liner element moves. This direction is conveniently defined by the angle δ between the velocity vector of the liner element and the perpendicular to the initial liner surface. We shall call δ the liner projection angle. For a fragmentation charge (or exploding bomb), the projection angle will determine the final angular distribution of the scattered fragments. For explosive cladding or shaped-charge liner collapse, it will determine the collapse angle β of the given charge. The specified qualities of either the cladding bond or the jet, crucially depend on this collapse angle.

A formula for determining the projection angle δ from the velocity of the liner V and the velocity U by which the detonation wave front sweeps past the liner surface was first proposed by Taylor [1]:

$$\sin\delta = V/2U \tag{1}$$

This formula, which has been the most extensively used one to date (see References 2-8), is, however, accurate only under steady state conditions where the detonation wave sweeps past identical cross sections of the explosive-liner geometry. For non-steady cases, the Taylor formula is not applicable since the existence of either a gradient, $\frac{\partial V}{\partial \ell}$, of the velocity V along the liner or a gradient, $\frac{\partial \tau}{\partial \ell}$, of the typical acceleration duration τ(ℓ denotes the length tangential to the liner surface) may very significantly affect the angle δ, sometimes causing very big deviations between the Taylor predictions and experimental measurements.

A more accurate formula for the liner projection angle is therefore needed. It will lead to a more accurate description and understanding of processes such as the collapse of the conventional shaped charge or the hemispherical liners and the formation of the self-forging fragment.

Recently, Randers-Pehrson [9] derived a non-steady liner projection angle formula by empirically fitting a formula to the numerically calculated results.

In the present paper an analytically derived formula is obtained. It is based on the assumptions that (1) the detonation pressure acts normally on the liner, and (2) the angle $(\theta-\delta)$, which will be defined later, is small.

We found that for the small angle assumption to be valid, the initial radius of curvature must be small in comparison with the distance traveled by the liner during acceleration. A third assumption is that the internal forces in the liner metal can be neglected. The new formula was tested against both numerical calculations and experimental data and was found to predict the projection angle δ more accurately than the steady Taylor formula.

In this report we address only the equation governing the angle δ and the velocity parameters V_0 and τ. No attempt is made here to determine values of V_0 and τ as functions of explosive and liner geometry and properties. It is obvious that values of V_0 and τ are needed for the eventual application of this equation. A simple method in determining V_0 and τ will be the objective of future research. For the present purpose of ascertaining the accuracy of the unsteady Taylor angle equation, we shall use values of V_0 and τ determined either by two-dimensional computer code, or by experimental measurement.

II. Derivation of Basic Equations

We shall first derive the differential equations describing the liner's motion. We shall limit ourselves to liners with very large initial radii of curvature. In other words, the liner has an almost straight formation line. The liner could either be an axisymmetric shell, or a "plane strain" plate. The explosion wave front is assumed to be cylindrically symmetric for the shell case with its axis of symmetry coinciding with that of the liner's. We denote by ℓ the length coordinate along the liner and by U the velocity by which the detonation wave front sweeps past the liner surface along the direction of the liner surface.

The first differential equation deals with the increase of liner velocity with time. Let V and δ be the magnitude and direction of the liner velocity at the point ℓ on the liner at a specific time, t. We make the assumption that the gas pressure always acts perpendicular to the liner surface. When a liner segment elongates or shrinks as it is pushed or pulled by its neighboring segments, a force component in the liner direction may also appear. We assume that this force can be neglected during the acceleration time. We denote by θ the angle between the original liner formation line direction and the current formation line direction, at ℓ. Then, we can see from Fig. 1 that the additional velocity vector $d\vec{V}$, at a given position ℓ, induced by the force acting perpendicularly to the liner during the time dt, adds to the current velocity vector $\vec{V}(t)$ to form the new velocity vector $\vec{V}(t+dt)$. As a result, the velocity increases in magnitude by the amount $dV = d|V| = |d\vec{V}| \cos(\theta-\delta)$ where $|d\vec{V}|$ is the magnitude of the above mentioned additional velocity vector. At the same time, the tangential velocity component $|d\vec{V}| \sin(\theta-\delta)$ causes the velocity direction to change by the angle $d\delta$. We can relate the angle $d\delta$ to this component by the equation:

$$|d\vec{V}| \sin(\theta-\delta) = V \cdot d\delta.$$

Substituting $|d\vec{V}| = dV/\cos(\theta-\delta)$ we get the scalar equation for the velocity magnitude:

$$dV \tan(\theta-\delta) = V \cdot d\delta \,. \tag{2}$$

Dividing by dt and denoting the differentiation with respect to the time by a dot above the symbol we finally obtain

$$\dot{\delta} = \frac{\dot{V}}{V} \tan(\theta-\delta) \,. \tag{3}$$

The next equation describes the influence of the existence of a velocity gradient along the liner. We make the assumption that a liner will not elongate while being accelerated, or that its elongation may be neglected.

We are interested in calculating the rate-of-change of liner slope $\frac{\partial\theta}{\partial t}$. Referring to Fig. 2, we note that during the time dt,

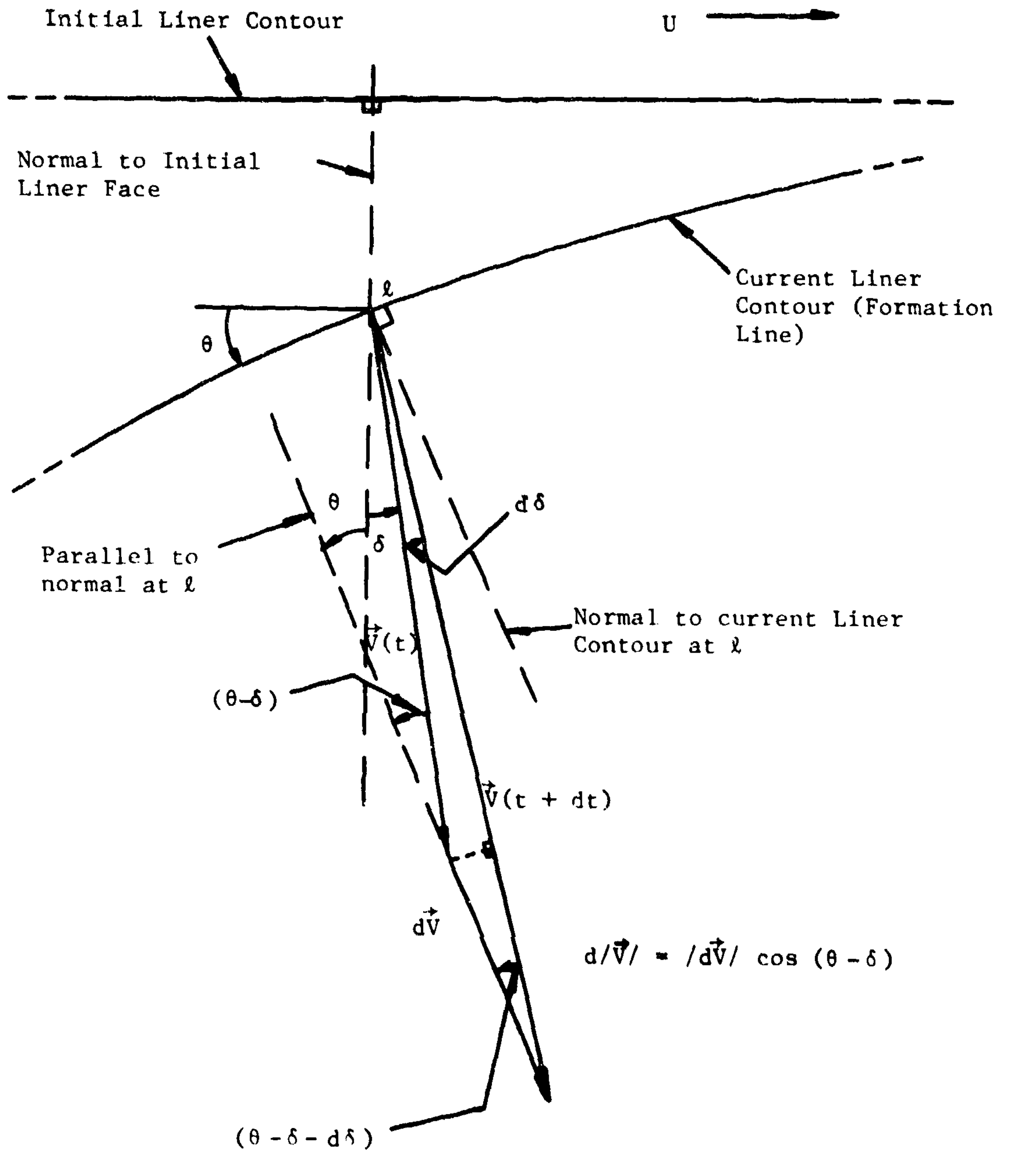

Figure 1. Liner acceleration diagram showing how the additional velocity $d\vec{V}$ contributes to the increase in magnitude and change in the direction of the current velocity, $\vec{V}$.

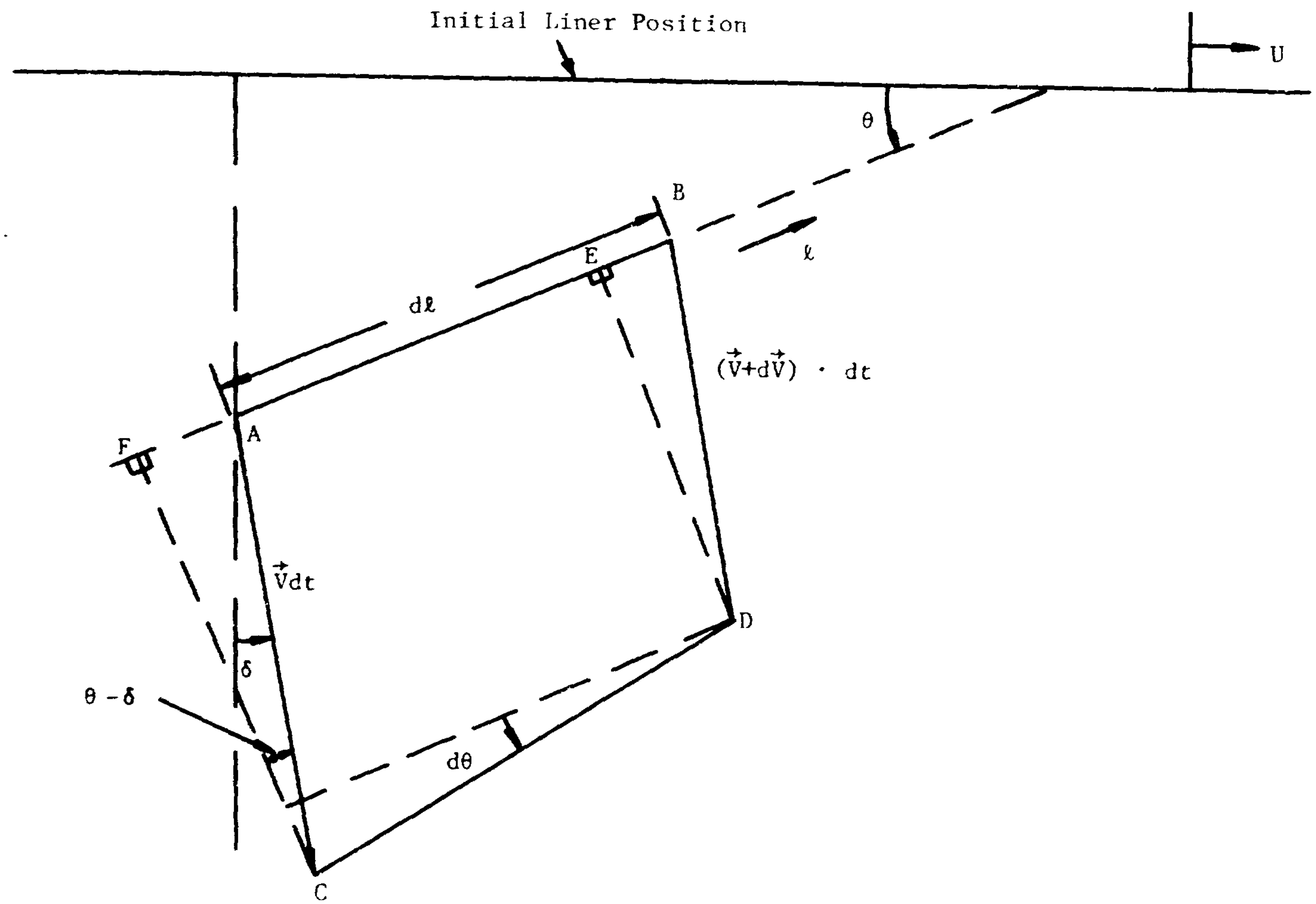

Figure 2. Liner position diagram showing the relation between its angular velocity and its linear velocity gradient.

point A will move the distance $V(t)dt$ to point C in a direction making the angle $\theta(\ell) - \delta(\ell)$ with the normal to the current liner surface at point A. Point B will move at the same time the distance $\left(V + \frac{\partial V}{\partial \ell} d\ell\right) \cdot dt$ to point D. The angle at A (see Fig. 2) between the initial and current liner direction is equal by definition to $\theta(\ell)$.

The angle $d\theta$ between CD and AB is determined by the components of $V\,dt$ and $(V + dV)dt$ normal to the current liner at ℓ thus:

$$d\theta \approx \tan(d\theta) = \frac{CF-DE}{d\ell} = \frac{[V-(V+dV)]\cos(\theta-\delta)}{d\ell}\,dt. \qquad (4)$$

At the limit of small $d\ell$ this yields:

$$\dot{\theta} = -\,V'\,\cos(\theta-\delta) \qquad (5)$$

where the prime denotes differentiation with respect to ℓ, and dot with respect to time.

III. Integration of Basic Equations

Eqs. (3) and (5) represent two equations governing the three quantities V, θ, and δ. Assuming that the spatial and temporal distribution of V for a given problem is known, we can solve for θ and δ. Under the approximation $\tan(\theta-\delta) \cong \theta-\delta$. Eq. (3) now becomes

$$\dot{\delta} + \frac{\dot{V}}{V} \cdot \delta = \frac{\dot{V}}{V} \theta. \tag{6}$$

Eq. (6) is a first order differential equation which for the initial conditions $\theta=\delta=V=0$ at $t \leq T$ has the general solution:

$$\delta = \frac{1}{V} \int_T^t \theta\dot{V} \, dt = \theta - \frac{1}{V} \int_T^t V\dot{\theta} \, dt \tag{7}$$

where T is the instant when the liner begins to accelerate. From Eq. (5) we obtain under the above approximation:

$$\theta = - \int_T^t V'\cos(\theta-\delta)\,dt \cong \int_T^t - V'dt. \tag{8a}$$

When we substitute $\dot{\theta}$ from Eq. (5), the second term of Eq. (7) becomes

$$- \frac{1}{V} \int_T^t V\dot{\theta}dt = \frac{1}{V} \int_T^t V\,V' \cos(\theta-\delta)\,dt \cong \frac{1}{V} \int_T^t VV'dt. \tag{8b}$$

We, therefore, obtain the general solution for δ

$$\delta = - \int_T^t V'dt + \frac{1}{2V} \int_T^t (V^2)'dt. \tag{9}$$

IV. Application to Exponential Acceleration

In order to apply Eq. (9) to a practical problem, we shall assume for V the exponential form:

$$V(\ell,t) = V_o(\ell)\left\{1 - \exp\left[-\left(\frac{t-T(\ell)}{\tau(\ell)}\right)\right]\right\} \qquad (10)$$

when V_0, T, and τ are functions of ℓ only. Though this form may not fit perfectly for all cases, it is reasonably accurate for cases we have studied and easily integrable for the calculation of δ given by Eq. (9). The corresponding acceleration is

$$a = \frac{\partial V}{\partial t} = \frac{V_0}{\tau}\exp\left[-\left(\frac{t-T}{\tau}\right)\right]$$

The quantity $T(\ell)$ is the arrival time of the detonation wave at the point ℓ on the liner, τ is the characteristic acceleration time of this point and $V_0(\ell)$ is the final asymptotic velocity reached by the liner. The time t=0 is taken when the detonation wave reaches a convenient point on the metal say ℓ=0.

To facilitate the integration, we interchange the order of time integration and differentiation with respect to ℓ.

$$\delta = -\frac{\partial}{\partial\ell}\int_T^t V\,dt + \frac{1}{2V}\frac{\partial}{\partial\ell}\int_T^t V^2 dt. \qquad (11)$$

(the differentiation with respect to T vanishes since V = 0 at t = T).

For the V function given by Eq. (10),

$$\int_T^t V\,dt = V_0(t-T) - \tau V \qquad (12)$$

$$\int_T^t V^2 dt = V_0[V_0(t-T) - \tau V] - \frac{1}{2}\tau V^2. \qquad (13)$$

Substituting Eq. (12) and (13) into Eq. (11) yields:

$$\delta = \frac{\partial}{\partial\ell}[\tau V - V_0(t-T)] - \frac{1}{2V}\frac{\partial}{\partial\ell}\{V_0[\tau V - V_0(t-T)] + \frac{1}{2}\tau V^2\}\ . \qquad (14)$$

To compare this equation with experimental results, we shall be interested in the value δ will obtain as $t \to \infty$. At this limit, V becomes equal to V_0, V' becomes equal to V_0' and the expression for δ becomes:

$$\delta = \frac{V_0 T'}{2} - \frac{1}{2}\tau V_0' + \frac{1}{4}\tau' V_0. \tag{15}$$

Let U be the detonation wave sweep speed, then T' is equal to 1/U for a detonation on the axis of symmetry and Eq. (15) becomes:

$$\delta = \frac{V_0}{2U} - \frac{1}{2}\tau V_0' + \frac{1}{4}\tau' V_0. \tag{16}$$

The first term is, for a small angle δ, identical to the Taylor formula, Eq. (1), and the other two are the correction terms.

V. Constant Acceleration Equation

In deriving Eq. (16) we assumed the exponential form for the velocity time dependence. Even though this form very well simulates the experimental measurements it is not the only form one can choose to fit the experimental data. When solving Eq. (9) with a constant acceleration assumption at the period of time $T < t \leq \left(T + \tau_c\right)$ i.e.,

$$V = V_0\left(\frac{t-T}{\tau_c}\right) \tag{17}$$

we find

$$\delta = \frac{V_0 T'}{2} - \frac{1}{6}\,\tau_c V_0{}' + \frac{1}{6}\,\tau_c{}'\ V_0 \tag{18}$$

and for the form:

$$V = V_0\left(\frac{t-T}{\tau_{SR}}\right)^{1/2} \tag{19}$$

we obtain

$$\delta = \frac{V_0 T'}{2} - \frac{1}{6}\,\tau_{SR}\ V_0{}' + \frac{1}{12}\,\tau_{SR}'\ V_0\,. \tag{20}$$

It can easily be seen that the τ_{SR} parameter of Eq. (19) exactly corresponds to 3τ, when τ is the corresponding parameter in the exponential acceleration (Eq. 10).

Using an acceleration form such as Eq. (17) or Eq. (19) may be more convenient in obtaining a closed form solution in more complicated cases, e.g., when the effect of the liner curvature on the angle δ cannot be neglected.

VI. Comparison with Previous Work and Two-Dimensional Code Calculations

Let us now compare Eq. (16) with the equation obtained empirically by Randers-Pehrson [9] using Two-D code calculations and experiment. The formula given in Ref. 9 is as follows:

$$\delta = \frac{V_0}{2U} - \frac{1}{2}\tau V_0' - \frac{1}{5}(\tau V_0')^2. \tag{21}$$

(Note that Eq. (21) agrees with Eq. (16) in the first two terms).

To perform this comparison we need to know V_0 and V_0', τ and τ'. There exists some experimental data for V_0 and V_0' from exploding cylinder tests. Experimental data for τ (except in special steady state cases) seems lacking, however. We, therefore, performed Two-D code simulations to calculate V_0, V_0', τ, τ' and δ for two specific geometries. Our general approach is to use output from a Two-D code of V_0 and τ at a number of ℓ locations to numerically calculate V_0' and τ'. Then substituting these values of V_0 and V_0', τ and τ' into Eq. (16), we obtain a value for δ which we shall denote δ_F (F - formula). The value of δ_F is then compared with the Two-D code value of δ denoted δ_c(c-code). Wherever experimental measurements of δ are available for a specific charge we shall denote them δ_{ex}. We expect to find a good agreement between δ_c and δ_{ex} when using a reliable Two-D code. Therefore, a check against experimental data is, in fact, a check of the Two-D code validating its use for checking Eq. (16). For completeness, these values are also substituted into Eq. (21) and the result denoted δ_{RP}

The two dimensional code we found most convenient to apply to this purpose is a Lagrangian code named TEMPS in which the explosive is treated by a two-dimensional finite-difference grid similar to HEMP, TOODY and other Two-D Lagrangian codes. The liner in TEMPS, however, is described as an array of mass points having tensile and bending forces between each two neighboring points. The liner is thus being treated as one-dimensional. This not only saves computation time but also facilitates the data reduction from the code output.

A. Conical Shaped Charge

The first configuration studied is the 81.3 mm diameter, 42°, conical shaped charge depicted in Fig. 3. In this example we choose ℓ=0 at the cone liner apex and ℓ is the distance from this point along the formation line. The charge is initiated by plane detonation at the rear of the explosive.

From the TEMPS code calculations, the velocity history for each liner mass-point position ℓ is recorded and plotted. A typical plot is shown in Fig. 4. The asymptotic final velocity reached is defined as $V_0(\ell)$ for each mass point. These are tabulated in Table 1 for this case. This final velocity is then plotted as a function of ℓ as shown in Fig. 5a. This curve is then numerically differentiated

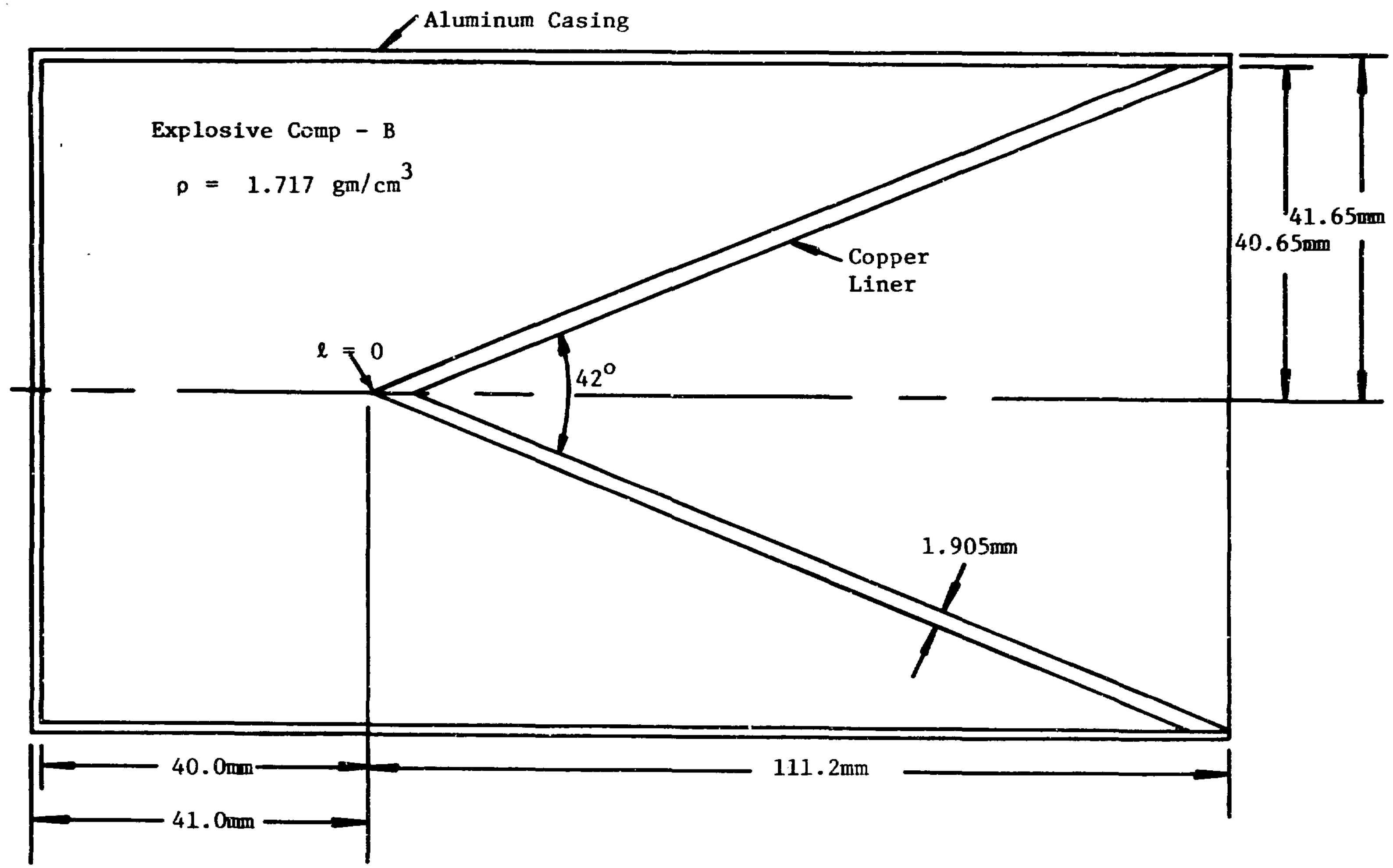

Figure 3. Drawing of 81.3mm diameter 42° conical shaped charge.

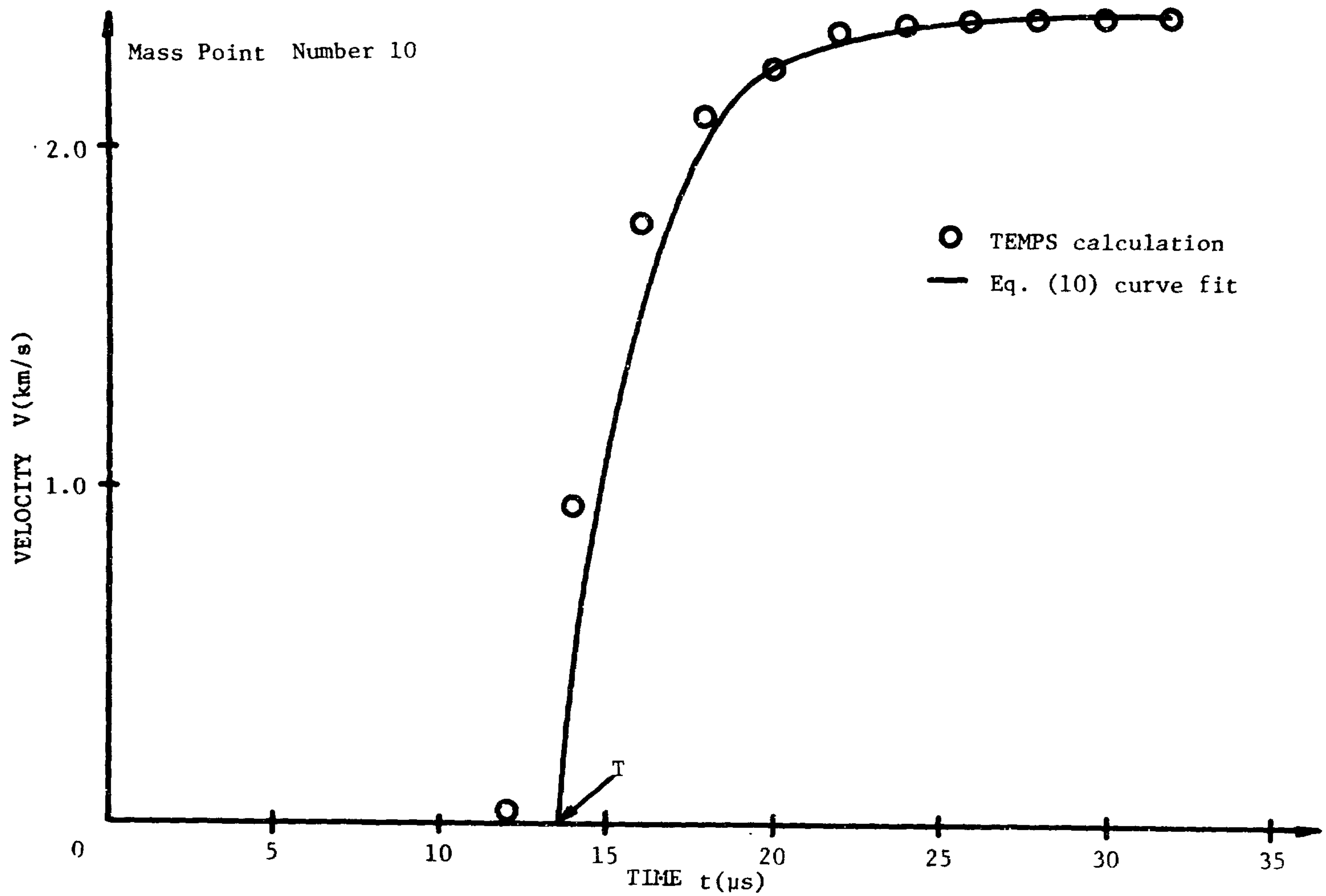

Figure 4. Fit of exponential velocity vs. time equation to the TEMPS computer code data for Mass Point number 10 (ℓ=73.64mm).

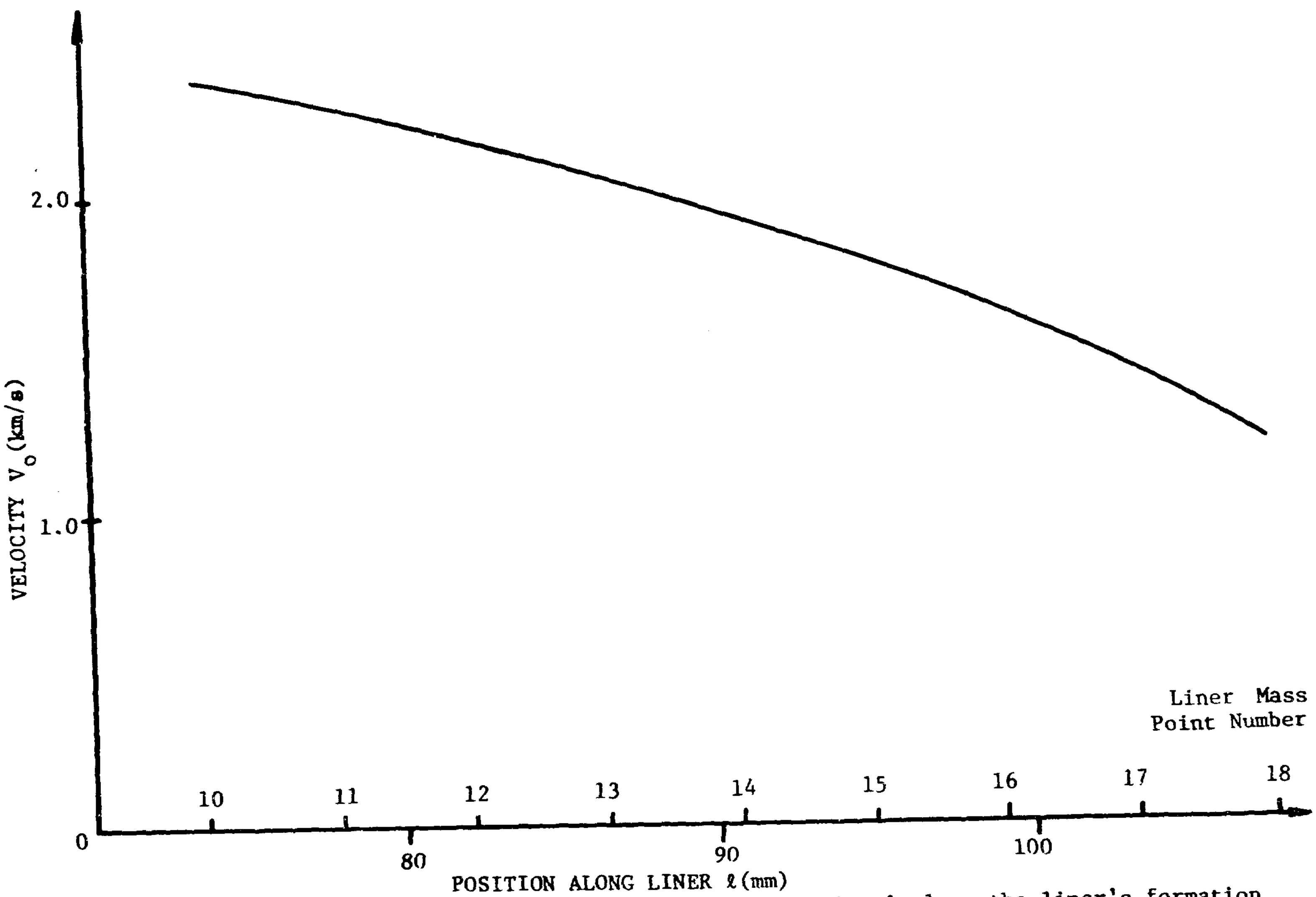

Figure 5a. Final velocity V_0 as a function of location ℓ along the liner's formation line.

TABLE 1. RESULTS OF 42° SHAPED CHARGE CALCULATIONS

Position ℓ along formation line (mm)	V_0 (km/s)	τ (μs)	V_0' (μs^{-1})	τ' (ms/m)	δ Taylor (degrees)	$\frac{-V_0'\tau}{2}$ (degrees)	$\frac{\tau' V_0}{4}$ (degrees)	$\frac{-(\tau V_0')^2}{5}$ (degrees)	δ_F Eq. (16) (degrees)	δ_{RP} Eq. (21) (degrees)	δ_c TEMPS Code (degrees)
73.64	2.387	2.375	-.0200	0.0	7.990	1.361	0.0	-.026	9.351	9.325	8.92
77.90	2.291		-.0267		7.669	1.814		-.046	9.483	9.437	9.18
82.17	2.173		-.0267		7.274	1.814		-.046	9.088	9.042	9.15
86.43	2.052		-.0320		6.869	2.177		-.066	9.046	8.980	9.15
90.69	1.915		-.0320		6.410	2.177		-.066	8.587	8.521	9.02
94.96	1.775		-.0333		5.942	2.268		-.072	8.209	8.138	8.66
99.22	1.625		-.0390		5.439	2.654		-.098	8.093	7.995	8.62
103.48	1.435		-.0478		4.803	3.251		-.148	8.054	7.907	8.73

using the simple difference formula $\Delta V_0/\Delta \ell$ to obtain $V_0'(\ell)$ which is also contained in Table 1.

Next we must estimate the value of τ for each mass point. This was obtained by fitting Eq. (10) to the TEMPS velocity data. The arrival time T used in Eq. (10) is the theoretical arrival time at the explosive metal interface and obtained by dividing the distance between the plane of initiation and the point ℓ by the detonation velocity U_D. As is indicated in Fig. 4, the wave arrival time predicted by the TEMPS code does not coincide with the calculated theoretical arrival time. This inaccuracy in the code simulation is caused by the code's smearing of the detonation front in the finite-difference calculation scheme. Therefore, in performing the fit for τ, we did not choose τ as the value of t when $V = V_0(1-e^{-1}) = 0.632\ V_0$, as is indicated by Eq. (10). This value of τ would be inaccurate since it is close to and heavily influenced by the code's calculation of wave arrival time. We found it more reliable to fit the curves closely in the region $V \geq .86\ V_0$. The values of τ obtained from this procedure are given in Table 1. These values of τ are also plotted as a function of ℓ in Fig. 5b. A line is fitted through the points and τ' calculated by simple numerical differentiation. The values are shown in Table 1. We see that for this charge τ is approximately constant and therefore τ' is a very small quantity.

These values are then substituted into Eq. (16) and Eq. (21) as well as Taylor's relation and compared to the code calculations. The quantity δ_c is the angle of the velocity vector as given by TEMPS when the liner reaches a final velocity V_0. The detailed data are given in Table 1 and plotted graphically in Fig. 6. We see that the Eq. (16) gives a significant improvement over the Taylor relation and agrees well with the TEMPS code. Note that since the last term in both Eqs. (16) and (21) is small, the difference between Eq. (16) and Eq. (21) is small for this example.

B. <u>Exploding Cylinder</u>

The second configuration studied is an exploding cylinder which is identical to the example used by Randers-Pehrson [9,10]. It consists of a steel pipe segment 101.6 mm in length and a diameter of 50.8 mm filled with OCTOL as shown in Fig. 7. For this example, direct experimental measurements of δ and V_0 are presented in Ref. 10. In these experiments, the expanding cylindrical pipe breaks into fragments. The speed and direction of motion of the fragments are measured by means of x-ray shadowgraphs taken at several predefined times. Similar experiments were also conducted in References 11 and 12.

To provide a complete verification of Eq. (16), however, the quantity τ is also needed. Since no acceleration data was measured in these experiments, we cannot provide an experimental value for τ and hence a full experimental verification of Eq. (16) at this point in time is not possible. In fact, as mentioned in the previous section, measurements of metal motion during acceleration have been reported for only a very special steady state case (see [13,14) in

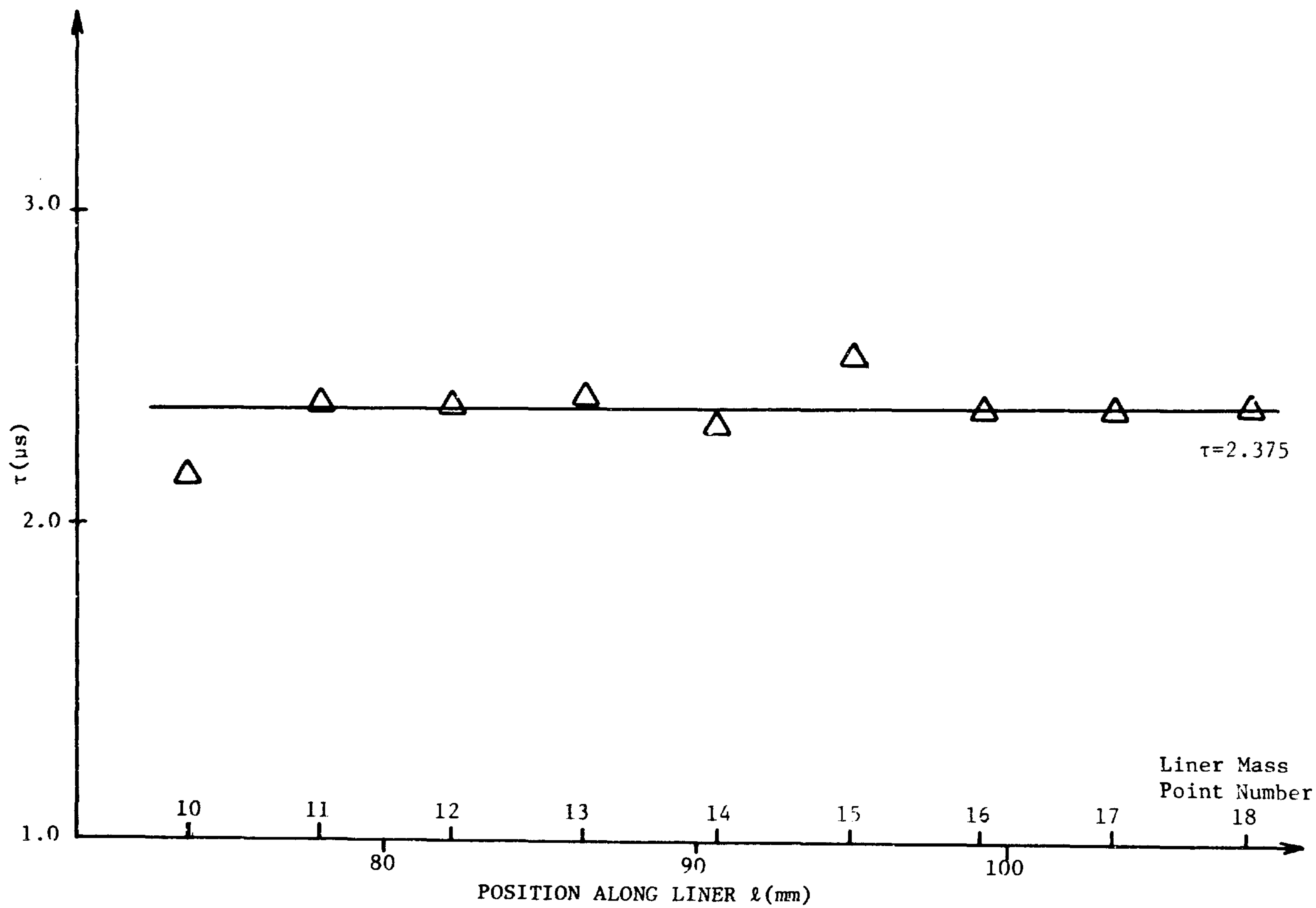

Figure 5b. Plot showing τ as a function of location ℓ from TEMPS calculation of the 42° conical charge.

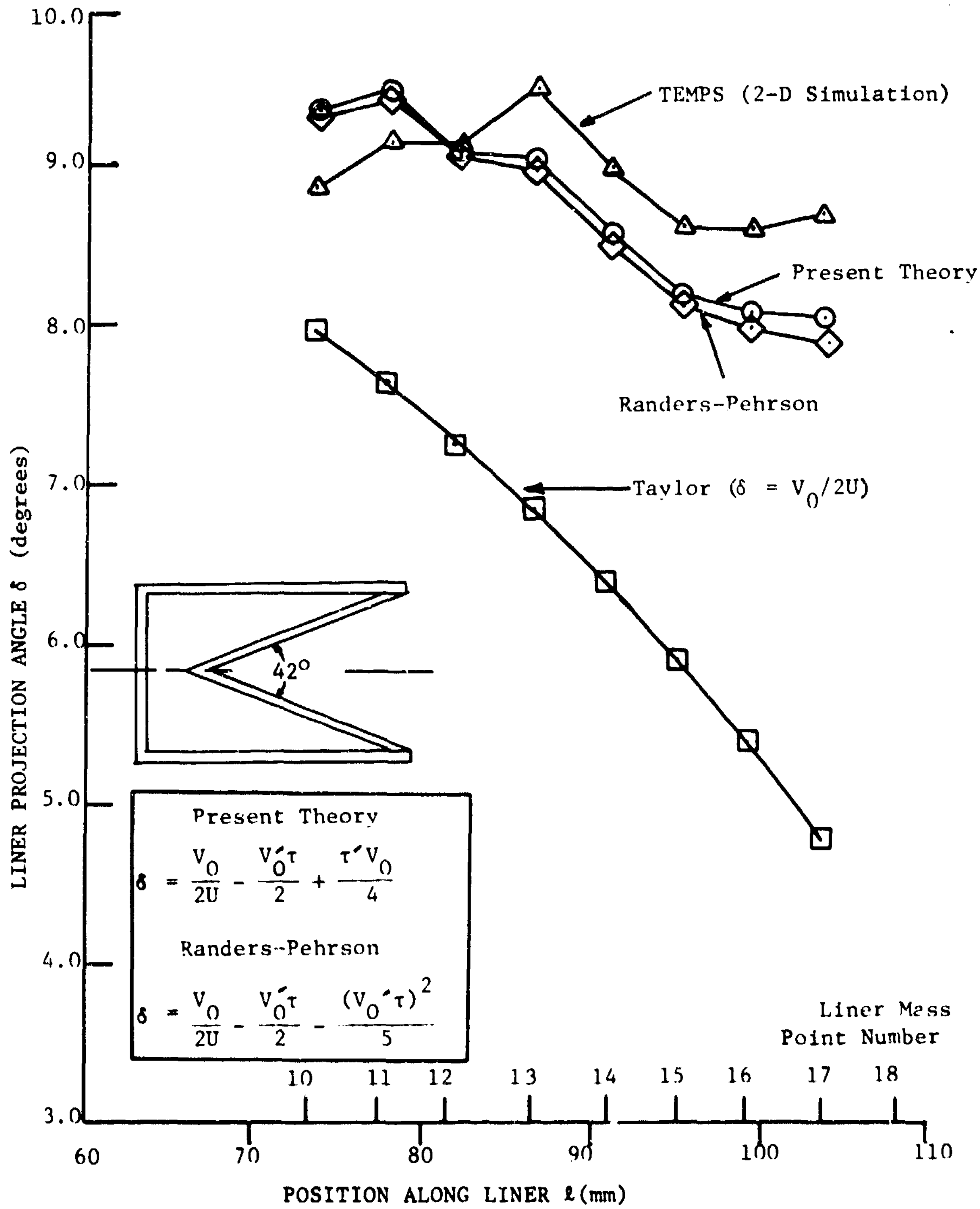

Figure 6. Comparison of the projection angle δ from formulas and two-dimensional calculations.

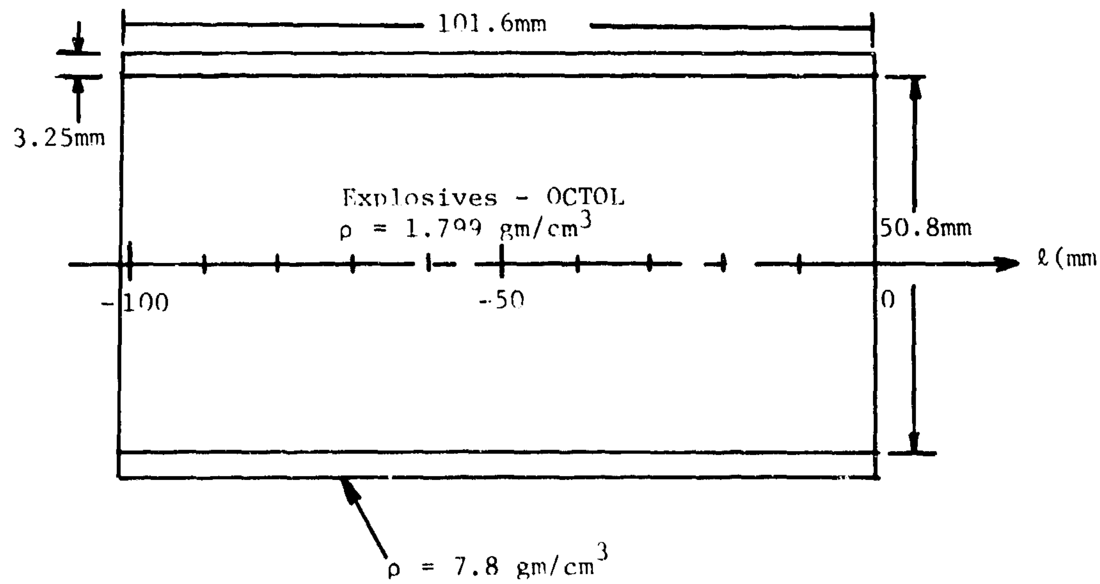

Figure 7. Exploding cylinder charge used for comparisons.

which V_0' and τ' are identically zero. Therefore, in our present comparison, TEMPS code calculations will again be used to supply the quantities τ and τ' (as well as V_0 and V_0'). The experimental data will thus be used to verify the final values for V_0 and δ given by the code calculations as well as the δ given by Eqs. (16) and (21).

The results of the TEMPS calculations for V_0 and δ are compared to the experimental data in Figs. 8 and 9. Also shown in these figures are the HEMP simulation results presented by Randers-Pehrson in [9]. Both TEMPS and HEMP results are within the spread of the experimental data.

The procedure to determine τ, τ', V_0 and V_0' from the TEMPS data was described in the previous section. A velocity vs. time plot for a typical mass point is shown in Fig. 10. A plot of τ vs. ℓ is given in Fig. 11. The values of all the necessary quantities are listed in Table 2. These values were then substituted into Eqs. (16) and (21) to compute δ_F and δ_{RP}. Fig. 12 is a comparison of δ_F, δ_{RP}, the Taylor formula and the TEMPS result δ_c. We see that considerable improvement in the estimation of the angle δ is achieved. Again, we note that the third term in both Eqs. (16) and (21) is small, therefore, δ_F and δ_{RP} do not differ significantly.

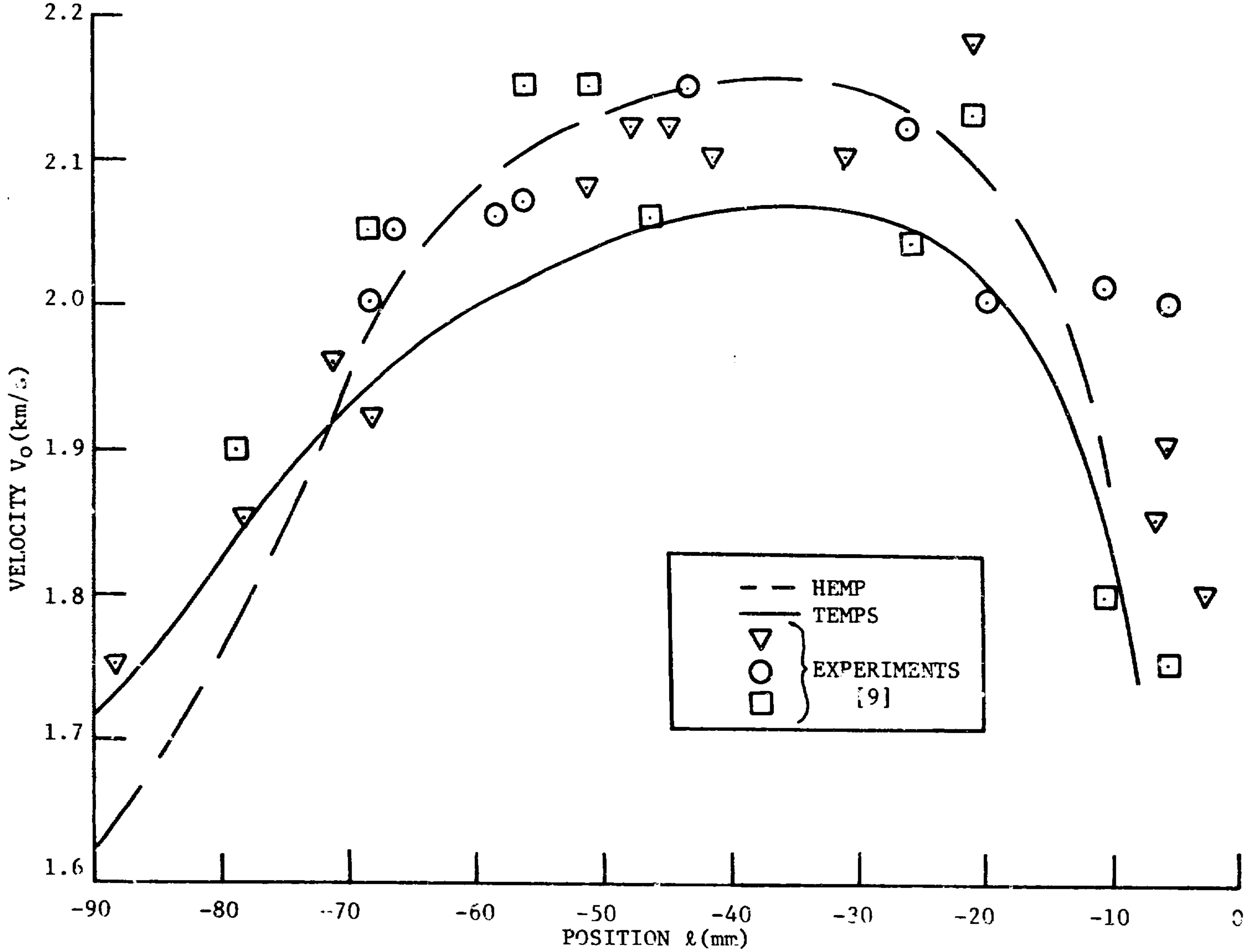

Figure 8. Comparison of TEMPS, HEMP and experimental data for V_o of an exploding cylinder.

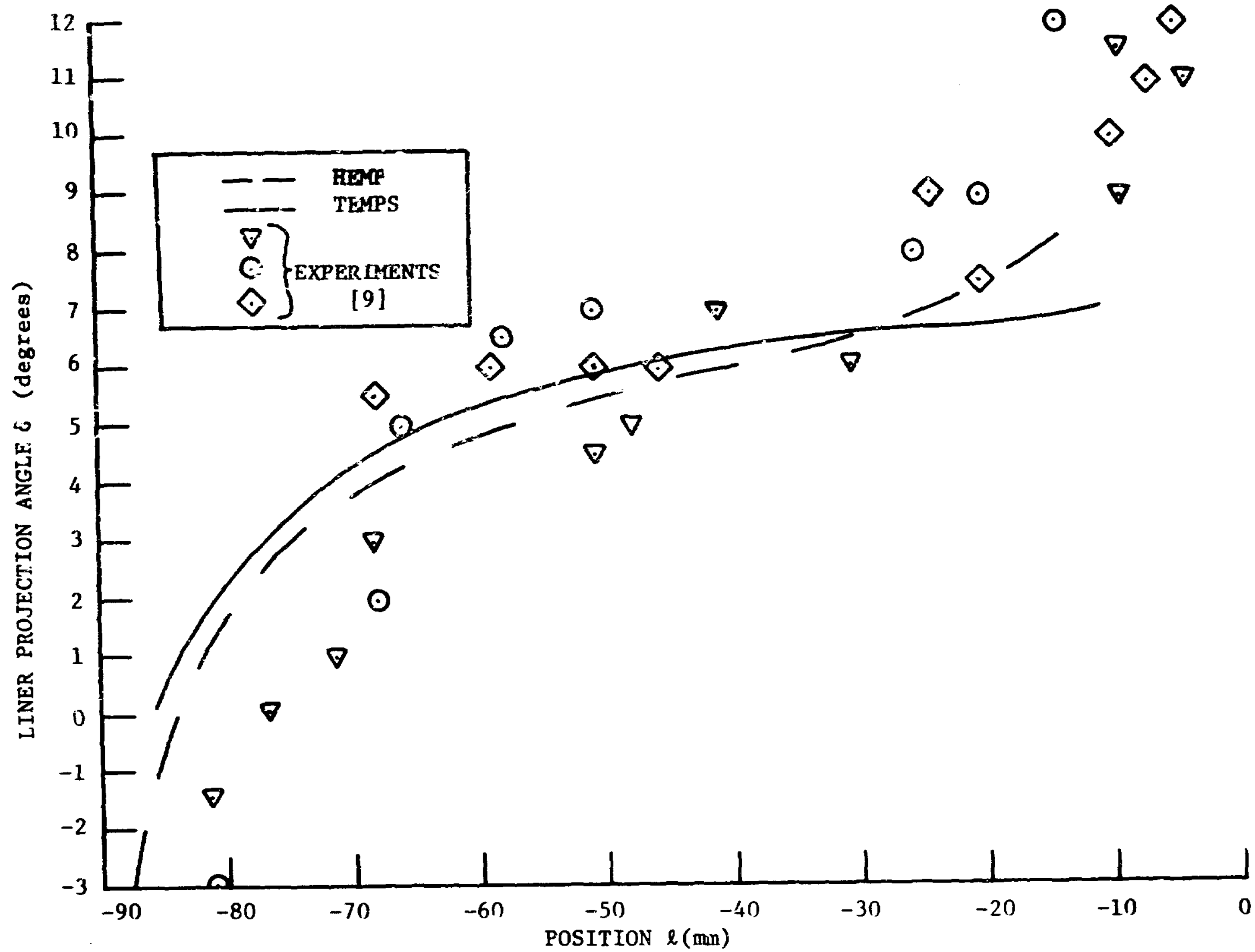

Figure 9. Comparison of TEMPS, HEMP, and experimental data for the liner projection angle δ of an exploding cylinder.

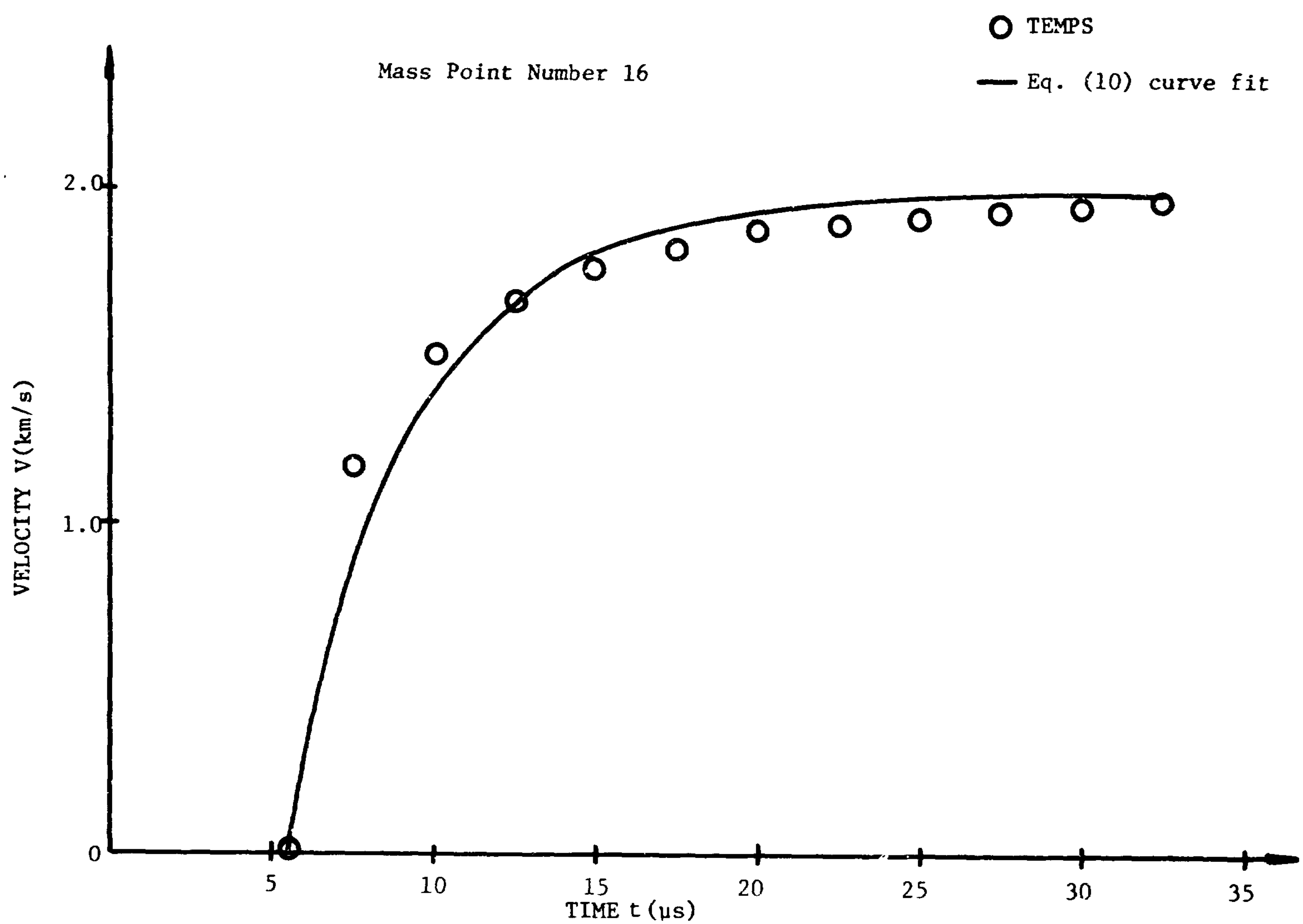

Figure 10. Exponential fit of TEMPS Mass Point velocity V vs. time at ℓ=-64.38mm.

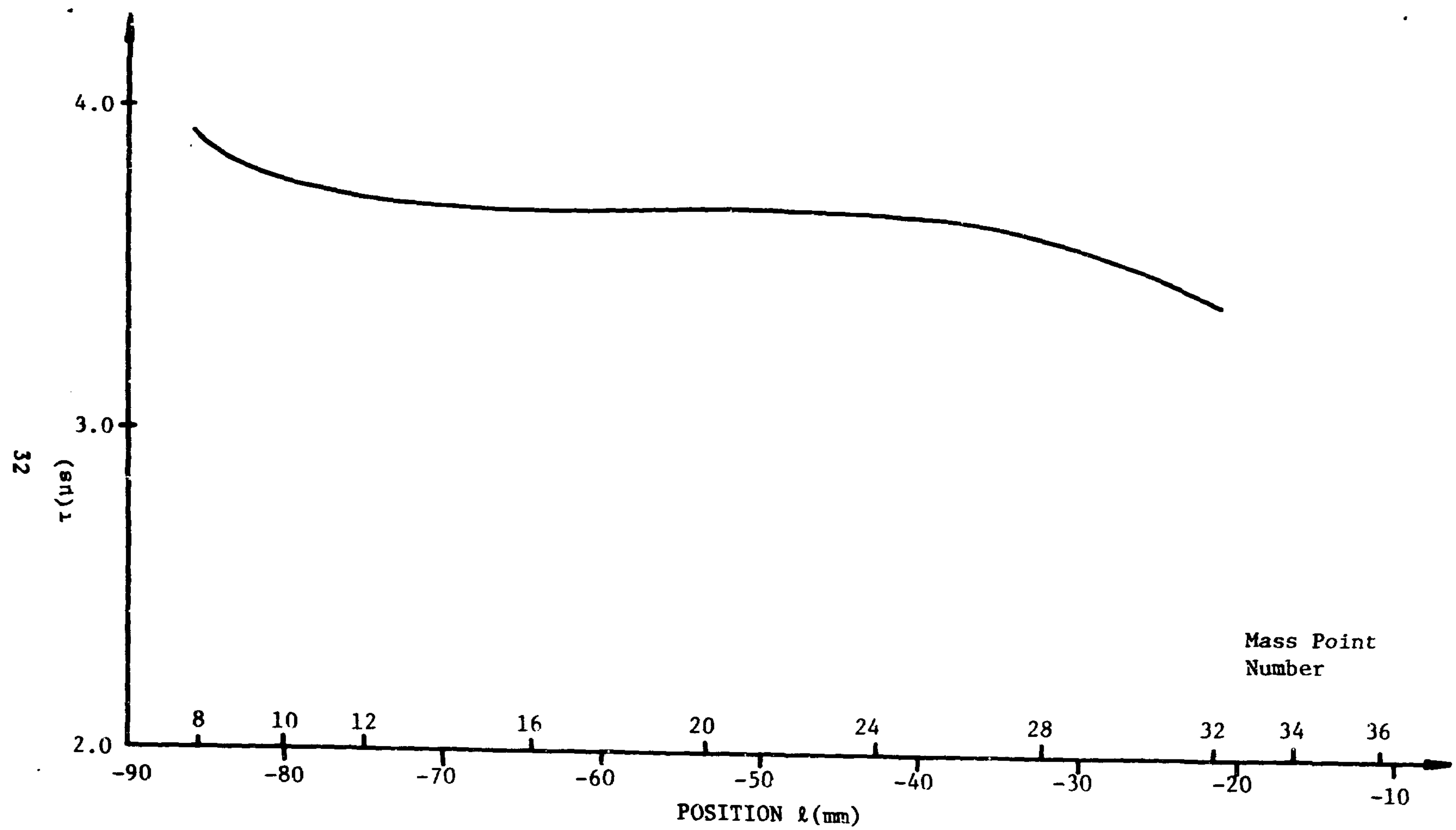

Figure 11. Plot showing τ as a function of location ℓ fitted from TEMPS calculation of exploding cylinder charge.

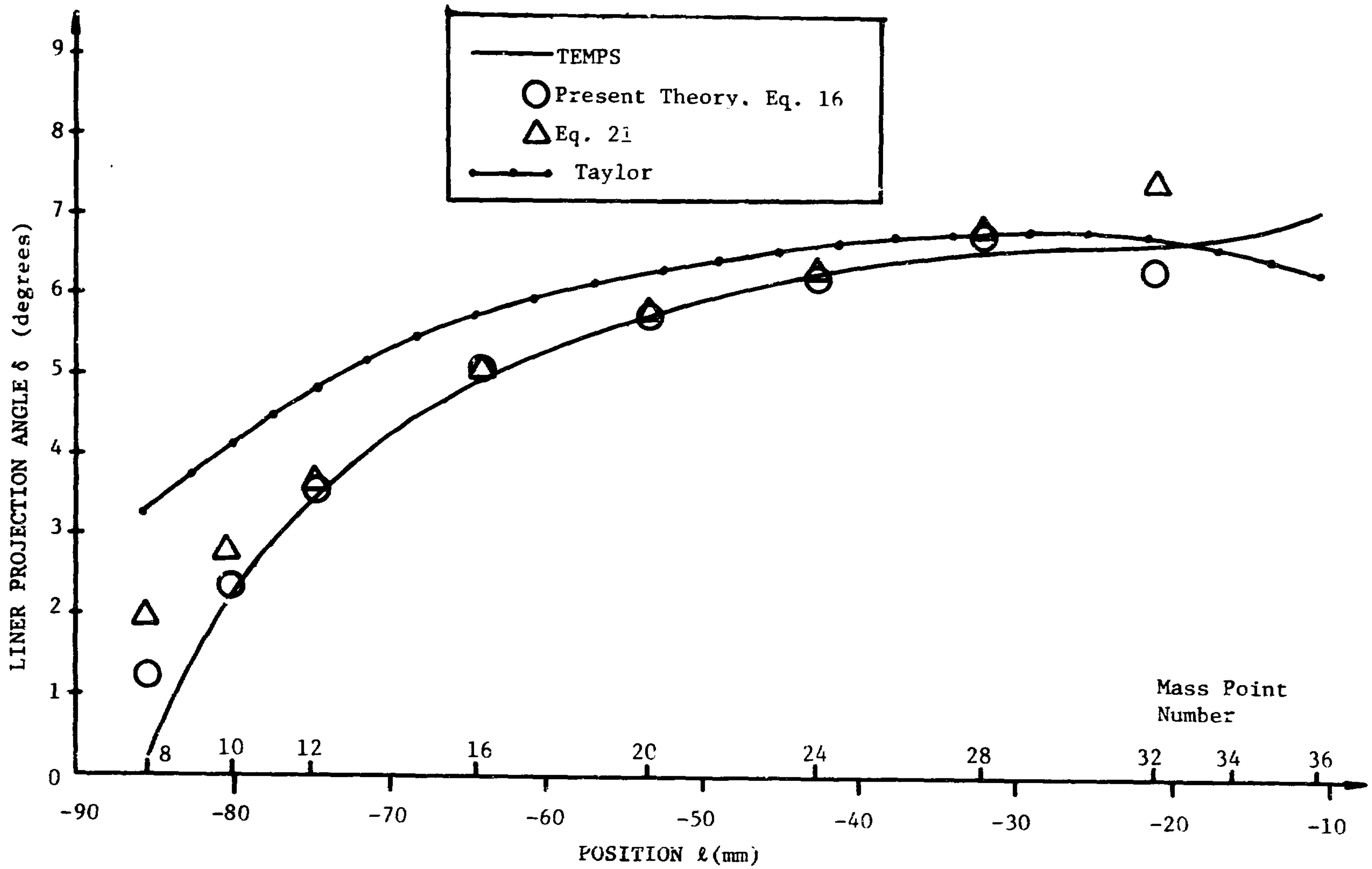

Figure 12. Comparison of projection angle δ calculated from formulas and TEMPS Code.

TABLE 2. RESULTS OF EXPLODING CYLINDER CALCULATIONS

Mass Point Number	V_0 $\left(\frac{km}{s}\right)$	V_0' (μs^{-1})	τ (μs)	τ' (ms/m)	δ_{Taylor} (degrees)	δ_{RP} Eq. 21 (degrees)	δ_F Eq. 16 (degrees)	δ_c TEMPS (degrees)
8	1.757	.0113	3.90	-.031	3.278	1.999	1.230	.13
10	1.824	.0121	3.76	-.018	4.106	2.774	2.319	2.22
12	1.885	.0100	3.71	-.006	4.774	3.695	3.549	3.48
16	1.972	.006	3.68	-.000	5.702	5.064	5.080	4.93
20	2.025	.004	3.68	-.002	6.258	5.814	5.747	5.78
24	2.058	.002	3.65	-.005	6.602	6.366	6.207	6.28
28	2.071	-.001	3.60	-.003	6.795	6.869	6.796	6.57
32	2.034	-.001	3.40	-.004	6.775	7.476	6.366	6.72

VII. Summary and Conclusions

In this report a formula for the explosive-metal Taylor angle δ in the unsteady case was derived from basic physical principles under the assumptions

(a) the explosive pressure always acts normal to the current liner surface.

(b) total angular motion of the metal is small (i.e., $\theta-\delta$ is small)

(c) forces in the liner are small during the acceleration time.

Also, the present case is restricted to liners whose meridional curvature is small. Under the assumption of an exponential decaying acceleration in time of the metal, this formula is given by

$$\delta = \frac{V_0}{2U} - \frac{1}{2}\tau V_0{}' + \frac{1}{4}\tau' V_0$$

where V_0 is the final velocity, τ the characteristic acceleration time, and U the detonation sweep speed; the prime indicates spatial differentiation along the liner. We point out that the first term represents the steady-state Taylor result. The remaining two terms represent the unsteady effects. Note that the first two terms are identical to the semi-empirical formula given in [9].

For the collapse of a conical shaped charge and the explosion of a metal cylinder we have found this formula to yield accurate results when compared to Two-D hydrocode calculations and to provide a significant improvement over the Taylor relation. The experimental data available also shows that the formula is accurate.

More recently, liners with large amounts of curvature in the meridional direction (formation line) such as hemispheres have shown promise as candidates for certain warhead applications. For such cases, the present formula is not applicable. It is therefore suggested that the current analysis be extended to include these more complex geometries.

Acknowledgement

The authors would like to thank Dr. William Walters and Mr. John Kineke of BRL for their valuable advice and comments and Mr. Richard Foedinger and Mr. Charles Dabundo of Dyna East Corporation for their assistance in the reduction of data from the simulations and for their assistance in the preparation of this document.

References

1. Taylor, G.I., "Analysis of the Explosion of a Long Cylindrical Bomb Detonated at One End," (1941), Scientific Papers of G.E. Taylor, Vol. III, Cambridge University Press, 1963, pp. 277-286.

2. Birkhoff, G., MacDougall, D.P., Pugh, E.M., and Taylor, G., "Explosives with Lined Cavities," J. Appl. Phys., Vol. 19, June 1948, pp. 563-582.

3. Pugh, E.M., Eichelberger, R.J. and Rostoker, N., "Theory of Jet Formation by Charges with Lined Conical Cavities," J. Appl. Phys., Vol. 23, No. 5, May 1952, pp. 532-536.

4. Eichelberger, R.J. and Pugh, E.M., "Experimental Verification of the Theory of Jet Formation by Charges with Lined Conical Cavities," J. Appl. Phys., Vol. 23, No. 5, May 1952, pp. 537-542.

5. Eichelberger, R.J., "Re-Examination of the Nonsteady Theory of Formation by Lined Cavity Charges," J. Appl. Phys., Vol. 26, No. 4, April 1955, pp. 398-402.

6. Hirsch, E., "A Simple Representation of the Pugh, Eichelberger and Rostoker Solution to the Shaped Charge Jet Formation Problem," J. Appl. Phys., Vol. 50, No. 7, July 1979, pp. 4667-4670.

7. Carleone, J. and Chou, P.C., "A One Dimensional Theory to Predict the Strain and Radius of Shaped Charge Jets." Proceedings of the First International Symposium on Ballistics. Orlando, Florida, November 13-15 (1976).

8. Defourneaux, M., "The Push Plate Test for Explosives," Proceedings of the First International Symposium on Ballistics. Orlando, Florida, November 13-15 (1976).

9. Randers-Pehrson, Glenn, "An Improved Equation for Calculating Fragment Projection Angle," Proceedings of 2nd International Symposium on Ballistics, Daytona Hilton, Daytona Beach, Florida, March 9-11 (1977).

10. Karpp, R.R., Kronman, S., Dietrich, A.M., and Vitali, R., "Influence of Explosive Parameters on Fragmentation," BRL Memorandum Report No. 2330, USA Ballistic Research Laboratory, Aberdeen Proving Ground, Maryland, October 1973. (AD #917248L)

11. Allison, F.E. and Watson, R.W., "Explosively Loaded Metallic Cylinders I," J. Appl. Phys., Vol. 31, No. 5, May 1960, pp. 842-845.

12. Allison, F.E. and Schriemf, J.T., "Explosively Loaded Metallic Cylinders II," J. Appl. Phys., Vol. 31, No. 5, May 1960, pp. 846-851.

13. Kury, J.W., Horning, H.C., Lee, E.L., McDonnell, J.L., Ornellos, D.L., Finger, M., Strange, F.M., Wilkins, M.L., "Metal Acceleration by Chemical Explosives," Fourth International Symposium on Detonation ONR ACR-126, 1965.

14. Bjarenholt, G.,"Effect of Aluminum and Lithium Flouride Admixtures on Metal Acceleration Ability of Comp. B," Proceedings of the 6th International Symposium on Detonation, Coronado, California, August 1976.

DISTRIBUTION LIST

No. of Copies	Organization
12	Commander Defense Technical Info Center ATTN: DDC-DDA Cameron Station Alexandria, VA 22314
1	Assistant Secretary of the Army (R&D) ATTN: Asst for Research Washington, DC 20310
2	HQDA (DAMA-ZA, DAMA-AR) Washington, DC 20310
1	Commander US Army Materiel Development and Readiness Command ATTN: DRCDMD-ST 5001 Eisenhower Avenue Alexandria, VA 22333
8	Commander US Army Armament Research and Development Command ATTN: DRDAR-TSS (2 cys) Mr. T. Stevens Mr. G. Randers-Pehrson Dr. N. Clark Mr. J. Hershkowitz Mr. J. Pearson LCU-CT, Mr. E. Yuhas Dover, NJ 07801
1	Commander US Army Armament Materiel Readiness Command ATTN: DRSAR-LEP-L, Tech Lib Rock Island, IL 61299
1	Director US Army ARRADCOM Benet Weapons Laboratory ATTN: DRDAR-LCB-TL Watervliet, NY 12189

No. of Copies	Organization
1	Commander US Army Aviation Research and Development Command ATTN: DRDAV-E 4300 Goodfellow Boulevard St. Louis, MO 63120
1	Director US Army Air Mobility Research and Development Laboratory Ames Research Center Moffett Field, CA 94035
1	Commander US Army Communications Rsch and Development Command ATTN: DRDCO-PPA-SA Fort Monmouth, NJ 07703
1	Commander US Army Electronics Research and Development Command Technical Support Activity ATTN: DELSD-L Fort Monmouth, NJ 07703
2	Commander US Army Missile Command ATTN: DRSMI-R DRSMI-YDL Redstone Arsenal, AL 35809
1	Commander US Army Tank Automotive Rsch and Development Command ATTN: DRDTA-UL Warren, MI 48090
2	Commander US Army Materials and Mechanics Research Center ATTN: DRXMR-RD, J. Mescall Tech Lib Watertown, MA 02172

DISTRIBUTION LIST

No. of Copies	Organization
1	Commander US Army Research Office P. O. Box 12211 Research Triangle Park NC 27709
1	Director US Army TRADOC Systems Analysis Activity ATTN: ATAA-SL, Tech Lib White Sands Missile Range NM 88002
2	Chief of Naval Research Department of the Navy ATTN: Code 427 Code 470 Washington, DC 20325
2	Commander Naval Air Systems Command ATTN: Code AIR-310 Code AIR-350 Washington, DC 20360
1	Commander Naval Ordnance Systems Command ATTN: Code ORD-0332 Washington, DC 20360
3	Commander Naval Surface Weapons Center ATTN: Code DG-50 DX-21, Lib Br N. Coleburn, R-13 Dahlgren, VA 22448
1	Commander Naval Surface Weapons Center ATTN: Code 730, Lib Silver Spring, MD 20910
2	Commander Naval Weapons Center ATTN: Code 3835 Code 3431, Tech Lib China Lake, CA 93555

No. of Copies	Organization
1	Commander Naval Research Laboratory Washington, DC 20375
1	USAF/AFRDDA Washington, DC 20311
1	AFSC/SDW Andrews AFB Washington, DC 20311
1	US Air Force Academy ATTN: Code FJS-41 (NC) Tech Lib Colorado Springs, CO 80840
1	AFATL/DLJR (J. Foster) Eglin AFB, FL 32542
1	AFWL (SUL, LT Tennant) Kirtland AFB, NM 87116
1	AFLC/MMWMC Wright-Patterson AFB, OH 45433
1	Director Lawrence Livermore Laboratory ATTN: Dr. J. Kury P. O. Box 808 Livermore, CA 94550
1	Director Lawrence Livermore Laboratory ATTN: Dr. M. Wilkins P. O. Box 808 Livermore, CA 94550
1	Director Lawrence Livermore Laboratory ATTN: Dr. E. Lee P. O. Box 808 Livermore, CA 94550

DISTRIBUTION LIST

No. of Copies	Organization
1	Director Lawrence Livermore Laboratory ATTN: Dr. H. Horning P. O. Box 808 Livermore, CA 94550
1	Director Lawrence Livermore Laboratory ATTN: Dr. J. Knowles P. O. Box 808 Livermore, CA 94550
1	Director Lawrence Livermore Laboratory ATTN: Dr. M. Van Thiel P. O. Box 808 Livermore, CA 94550
1	Director Lawrence Livermore Laboratory ATTN: Dr. C. Godfrey P. O. Box 808 Livermore, CA 94550
1	Director Lawrence Livermore Laboratory ATTN: Tech Lib P. O. Box 808 Livermore, CA 94550
1	Battelle-Columbus Laboratories ATTN: Mr. Joseph E. Backofen 505 King Avenue Columbus, OH 43201
2	Dyna East Corporation ATTN: P. C. Chou J. Carleone 227 Hemlock Road Wynnewood, PA 19096

No. of Copies	Organization
1	Firestone Defense Research and Products Division of the Firestone Tire and Rubber Company ATTN: R. Berus 1200 Firestone Parkway Akron, OH 44317
2	Honeywell, Inc. Government and Aeronautical Products Division ATTN: C. R. Hargreaves R. S. Kensinger 600 Second Street Hopkins, MN 55343
2	Sandia Laboratories ATTN: Dr. W. Herrman Dr. J. Asay Albuquerque, NM 87115
1	Shock Hydrodynamics ATTN: Dr. L. Zernow 4710-4716 Vineland Avenue North Hollywood, CA 91602
1	Systems, Science & Software ATTN: Dr. R. Sedgwick P. O. Box 1620 La Jolla, CA 92037
4	University of California Los Alamos Scientific Lab ATTN: Dr. J. Walsh Dr. R. Karpp Dr. C. Mautz Tech Lib P. O. Box 1663 Los Alamos, NM 87545
1	University of Denver Denver Research Institute ATTN: Mr. R. F. Recht 2390 S. University Blvd. Denver, CO 80210

DISTRIBUTION LIST

No. of Copies	Organization
2	University of Illinois Dept of Aeronautical and Astronautical Engineering ATTN: Prof. A. R. Zak Prof. S. M. Yen Urbana, IL 61801

Aberdeen Proving Ground

Dir, USAMSAA
ATTN: DRXSY-D
B. Oeheil
G. Johnson
DRXSY-MP, H. Cohen
Cdr, USATECOM
ATTN: DRSTE-TO-F
Dir, USACSL
Bldg. E3516, EA
ATTN: DRDAR-CLB-PA

USER EVALUATION OF REPORT

Please take a few minutes to answer the questions below; tear out this sheet, fold as indicated, staple or tape closed, and place in the mail. Your comments will provide us with information for improving future reports.

1. BRL Report Number ____________________________

2. Does this report satisfy a need? (Comment on purpose, related project, or other area of interest for which report will be used.)

____

____

____

3. How, specifically, is the report being used? (Information source, design data or procedure, management procedure, source of ideas, etc.) ____________________________

____

____

4. Has the information in this report led to any quantitative savings as far as man-hours/contract dollars saved, operating costs avoided, efficiencies achieved, etc.? If so, please elaborate.

____

____

5. General Comments (Indicate what you think should be changed to make this report and future reports of this type more responsive to your needs, more usable, improve readability, etc.) __________

____

____

____

6. If you would like to be contacted by the personnel who prepared this report to raise specific questions or discuss the topic, please fill in the following information.

Name: ____________________________

Telephone Number: ____________________________

Organization Address: ____________________________

____

____